AMERICAN SOCIETY FOR MICROBIOLOGY | Clinical and Vaccine Immunology®

CLINICAL IMMUNOLOGY

Combined Action of Human Commensal Bacteria and Amorphous Silica Nanoparticles on the Viability and Immune Responses of Dendritic Cells

Giulia Malachin,[a]* Elisa Lubian,[b] Fabrizio Mancin,[b] Emanuele Papini,[a] Regina Tavano[a]

Department of Biomedical Sciences, University of Padua, Padua, Italy[a]; Department of Chemical Sciences, University of Padua, Padua, Italy[b]

ABSTRACT Dendritic cells (DCs) regulate the host-microbe balance in the gut and skin, tissues likely exposed to nanoparticles (NPs) present in drugs, food, and cosmetics. We analyzed the viability and the activation of DCs incubated with extracellular media (EMs) obtained from cultures of commensal bacteria (*Escherichia coli*, *Staphylococcus epidermidis*) or pathogenic bacteria (*Pseudomonas aeruginosa*, *Staphylococcus aureus*) in the presence of amorphous silica nanoparticles (SiO_2 NPs). EMs and NPs synergistically increased the levels of cytotoxicity and cytokine production, with different nanoparticle dose-response characteristics being found, depending on the bacterial species. *E. coli* and *S. epidermidis* EMs plus NPs at nontoxic doses stimulated the secretion of interleukin-1β (IL-1β), IL-12, IL-10, and IL-6, while *E. coli* and *S. epidermidis* EMs plus NPs at toxic doses stimulated the secretion of gamma interferon (IFN-γ), tumor necrosis factor alpha (TNF-α), IL-4, and IL-5. On the contrary, *S. aureus* and *P. aeruginosa* EMs induced cytokines only when they were combined with NPs at toxic concentrations. The induction of maturation markers (CD86, CD80, CD83, intercellular adhesion molecule 1, and major histocompatibility complex class II) by commensal bacteria but not by pathogenic ones was improved in the presence of noncytotoxic SiO_2 NP doses. DCs consistently supported the proliferation and differentiation of $CD4^+$ and $CD8^+$ T cells secreting IFN-γ and IL-17A. The synergistic induction of CD86 was due to nonprotein molecules present in the EMs from all bacteria tested. At variance with this finding, the synergistic induction of IL-1β was prevalently mediated by proteins in the case of *E. coli* EMs and by nonproteins in the case of *S. epidermidis* EMs. A bacterial costimulus did not act on DCs after adsorption on SiO_2 NPs but rather acted as an independent agonist. The inflammatory and immune actions of DCs stimulated by commensal bacterial agonists might be altered by the simultaneous exposure to engineered or environmental NPs.

KEYWORDS nanoparticle toxicity, commensal and pathogenic bacteria, DC maturation, cytokines

Assessment of the possible interference of nanomaterials with host mechanisms dedicated to fighting infections or to immune tolerance is critical (1–3). In fact, the inhalation or the ingestion of various nanomaterials present in industrial, cosmetic, pharmacological, and food products or released by several anthropic activities or their contact with the skin may induce local alterations of the inflammatory and immune balance in tissues. Nanoparticles (NPs) also likely translocate from the respiratory or gastrointestinal mucosae to other organs via the blood (1, 2). In addition, the delivery of nanotheranostic agents through the mucosae and the skin may become an important route of administration in addition to intravenous injection (4, 5). Indeed, several

Received 6 June 2017 **Returned for modification** 29 June 2017 **Accepted** 13 August 2017

Accepted manuscript posted online 23 August 2017

Citation Malachin G, Lubian E, Mancin F, Papini E, Tavano R. 2017. Combined action of human commensal bacteria and amorphous silica nanoparticles on the viability and immune responses of dendritic cells. Clin Vaccine Immunol 24:e00178-17. https://doi.org/10.1128/CVI.00178-17.

Editor Helene F. Rosenberg, IIS/LAD/NIAID/NIH

Address correspondence to Emanuele Papini, emanuele.papini@unipd.it, or Regina Tavano, regina.tavano@unipd.it.

* Present address: Giulia Malachin, Department of Basic Sciences and Aquatic Medicine, Faculty of Veterinary Medicine and Biosciences, Norwegian University of Life Sciences, Oslo, Norway.

studies have indicated that dendritic cells (DCs) and macrophages, which are especially abundant in the mucosae and the skin, not only undergo oxidative stress, necrosis, and apoptosis but also overexpress T lymphocyte-stimulating proteins, such as major histocompatibility complex class II (MHC-II), CD80, and CD86, and secrete several proinflammatory cytokines and chemokines when they are treated with a variety of NPs (mesoporous silica NPs [SiO_2 NPs], TiO_2 NPs, and silica-coated iron dioxide and TiO_2 NPs) (6–17). Consistent with that finding, in mouse models, various modified silica NPs increased the efficacy with which DCs induced the differentiation of gamma interferon (IFN-γ)-producing $CD8^+$ T lymphocytes (Tc1), a phenotype linked with tissue inflammatory diseases, such as delayed-type hypersensitivity (DTH), characterized by macrophage and polymorphonuclear leukocyte (PMN) infiltration (18). Moreover, mouse bone marrow DCs treated with SiO_2 NPs were found to produce reactive oxygen species (ROS), which in turn triggered purinergic signaling, caspase-1 activation, and interleukin-1β (IL-1β) and IL-18 release (19). Eventually, it was found that the proinflammatory role of silica-loaded DCs is central in the pathogenesis of silicosis (20), and NP-stimulated Th2 humoral responses may exacerbate hypersensitivity to allergens (21).

All these studies indicate the effects of NPs on immune-regulatory cells in host tissue interfacing with the external environment and open the possibility, at present poorly understood, that microbial factors modulate the effects of NPs on tissues by altering the function of local immune/inflammatory leukocytes. In fact, not only pathogenic microorganisms but also commensal and symbiont microorganisms (organisms making up the microbiome) are especially present in those tissues prone to NP exposure, like the mucosae and the skin. Since the reciprocal interactions between the microbiome and the immune system (22–24) influence a delicate balance of defensive/proinflammatory and tolerance/anti-inflammatory responses (25–30), the presence of NPs may represent a factor perturbing host-microbe interactions and, in the end, tissue homeostasis. Such a possibility is indeed suggested by the little evidence that is available: endocytosed NPs and the lipopolysaccharide (LPS) of Gram-negative bacteria synergistically increase the levels of cytokine production by monocytes, macrophages, and DCs (17, 31–36) and cytotoxicity in A549 epithelial cells (37). In addition, prokaryotic agonists of formyl peptide receptors (FPRs) synergize with different NP types [SiO_2 NPs, bare or pegylated organically modified silica NPs, poly(lactic-coglycolic acid) NPs, and liposomes] in determining specific inflammatory responses in monocytes and PMNs (38, 39).

The hypothesis emerging from these considerations and data is essentially that the mechanism underlying NP-induced inflammation in the airway and gastrointestinal mucosae or the skin may involve not only the direct stimulation of innate inflammatory cells and cell damage but also alteration of the balance of the DC-mediated proinflammatory (Th1, Th17, and Tc1) or anti-inflammatory (regulatory T cell) response due to microbial factors and antigens.

To test this idea, we measured the mutual modulatory effects of SiO_2 NPs and diluted extracellular medium (EM) from selected bacteria on human DCs. This choice of NP is based on the fact that the mean human adult intake of amorphous silica, which is used as a drug excipient or as a food additive and which is used for these purposes at concentrations ranging from 3 to 15 μg/g of product (40), is estimated to be about 2 mg/kg of body weight/day (41). Although the nanosize nature of this material needs to be clarified (42), experiments suggest that SiO_2 NPs can enter intestinal epithelial cells and diffuse to the undermucosa or to the skin dermis (43–46), where they may induce anaphylactic reactions (47, 48). SiO_2 NPs are reported to induce cytotoxic, proinflammatory, and proimmune effects in murine DCs and skin Langerhans cells *in vitro* and *in vivo* (9, 49, 50). The Gram-negative bacterium *Escherichia coli* and the Gram-positive bacterium *Staphylococcus epidermidis* were chosen for use in this study because they are major commensals in the human gut and skin, respectively, while the Gram-negative bacterium *Pseudomonas aeruginosa* and the Gram-positive bacterium *Staphylococcus aureus* were employed because of their large diffusion in human bacterial infectious disease and ability to act as pathogenic/opportunistic agents. The

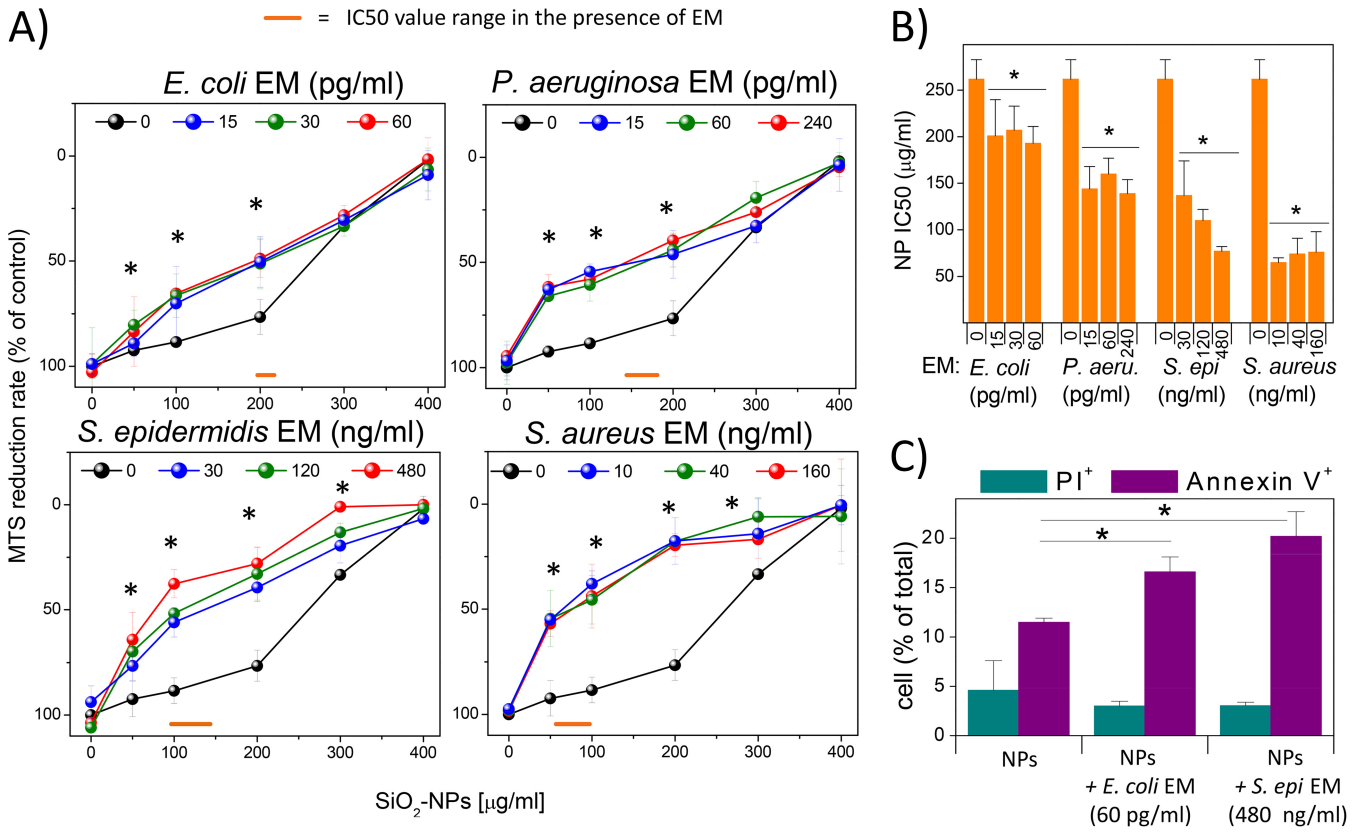

FIG 1 DC cytotoxicity induced by bacterial EMs and silica NPs. (A) DCs were incubated for 24 h with different NP concentrations in the presence or absence of the indicated EMs. The supernatants were aspirated, and cells were incubated with MTS solution until color development. The percent MTS reduction was calculated with respect to the amount for nontreated cells (control). Data are the means ± SEs ($n = 3$, run in triplicate). *, $P < 0.05$ with respect to cells not treated with EMs. (B) IC_{50} (SiO_2 NP doses resulting in 50% of the maximal cytotoxic effect, as measured by the MTS assay) values were plotted against EM concentrations. Data are means ± SEs ($n = 3$, run in triplicate). *, $P < 0.05$ with respect to cells treated with NPs alone. (C) DCs, treated as described above, were stained with annexin V-FITC and propidium iodide (PI) and subsequently subjected to FACS analysis. Bars represent the mean percentage ± SE ($n = 3$) for assays run in triplicate of PI-positive or annexin V-positive cells. *, $P < 0.05$ with respect to cells treated with NPs alone.

conditioned media from cultures of these bacteria were produced in a standardized manner and serially diluted to the point that their intrinsic activity was absent or suboptimal. We decided to use a cell-free mixture of molecules from bacterial cultures to mimic as close as possible the ensemble of potentially diffusible signals which may reach subepithelial DCs *in vivo* but that act at a distance from the bacterial cells producing these signals. The nanotoxicological and pathophysiological implications of the effects that were found correlated with the bacterial species (commensal or pathogenic) and the NP doses and are discussed.

RESULTS

Bacterium-derived factors and SiO_2 NPs synergistically induce cytotoxicity in DCs. DCs were coincubated for 24 h with NPs (concentration range, 25 to 400 μg/ml; see Fig. S1 in the supplemental material for transmission electron microscopy [TEM] images of the nanoparticles) and bacterial extracellular media (EMs) from *E. coli*, *P. aeruginosa*, *S. epidermidis*, and *S. aureus* at three dilutions lacking toxic and cytokine-inducing activity on DCs (Table S1 and Fig. S2). Their viability was then measured by 3-(4,5-dimethylthiazol-2-yl)-5-(3-carboxymethoxyphenyl)-2-(4-sulfophenyl)-2H-tetrazolium (MTS) tests. The results (Fig. 1A and B) showed that the toxicity of NPs, when used alone as an agonist (50% inhibitory concentration [IC_{50}] = 260 μg/ml), was moderately increased upon coincubation with EMs from the Gram-negative species *E. coli* (~1.3-fold toxicity increase; IC_{50} range = 193 to 207 μg/ml) and *P. aeruginosa* (~1.8-fold toxicity increase; IC_{50} range = 139 to 160 μg/ml). Stronger improvements in the cytotoxic effects of NPs were instead obtained when DCs were

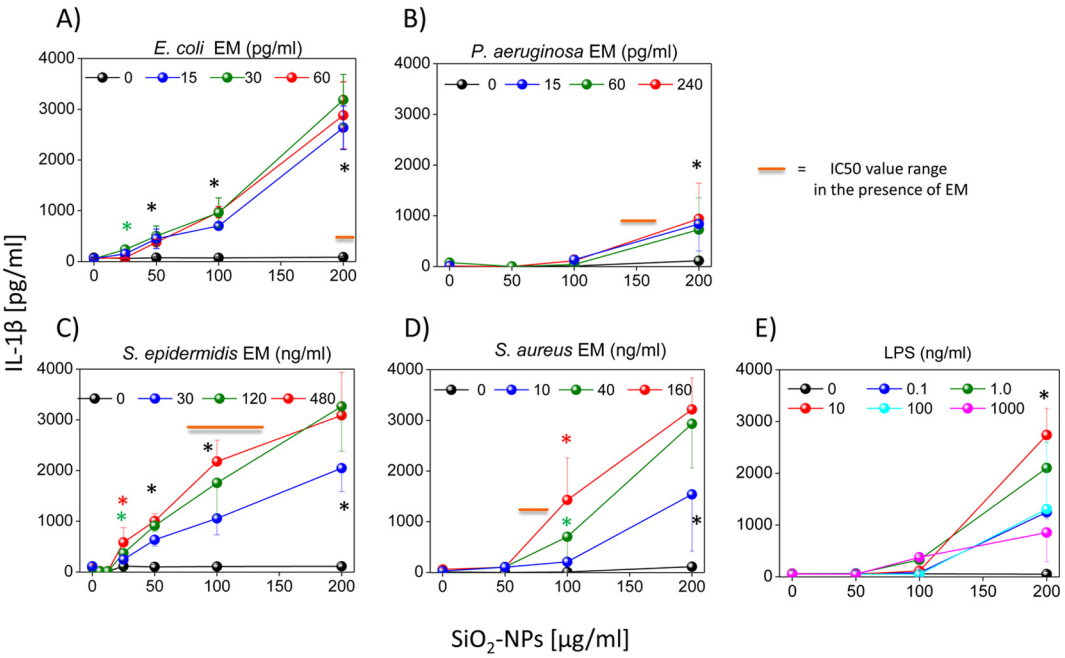

FIG 2 Coincubation of DCs with SiO_2 NPs and bacterium-derived EMs induces the release of IL-1β. DCs were incubated for 24 h with different concentrations of SiO_2 NPs and the culture supernatants (EMs) from different Gram-negative bacteria (A and B) or Gram-positive bacteria (C and D) or *E. coli* LPS as a positive control (E). The level of extracellular IL-1β was measured by ELISAs. Data are the means ± SEs ($n = 4$, performed in triplicate). Black asterisks, $P < 0.05$ with respect to cells treated with NPs alone for all EM concentrations used; green or red asterisks, $P < 0.05$ with respect to cells treated with NPs alone for the indicated concentration of EMs (indicated by the green and red symbols, respectively).

incubated with EMs from the Gram-positive bacteria *S. epidermidis* (~2.5-fold toxicity increase; IC_{50} range = 77 to 137 μg/ml) and *S. aureus* (3.7-fold toxicity increase; IC_{50} range = 65 to 76 μg/ml). Fluorescence-activated cell sorting (FACS) analysis showed a higher percentage of annexin V-positive cells than propidium iodide (PI)-positive ones in the populations treated with NPs and EMs from *E. coli* and *S. epidermidis*, suggesting the synergistic induction of apoptosis (Fig. 1C).

Different patterns of cytokine secretion were synergistically induced in DCs costimulated with SiO_2 NPs and bacterial factors. All EMs from the tested bacteria synergized the production of the major proinflammatory cytokine IL-1β, but with different efficacies and different levels of dependence on the NP dose-response. If we consider the Gram-negative bacteria (Fig. 2A and B), *E. coli* EMs synergized the production of IL-1β (NP concentration threshold, ~25 μg/ml; maximal level of cytokine production, ~2,800 pg/ml) much more intensely than *P. aeruginosa* EMs (NP concentration threshold, ~100 μg/ml; maximal level of cytokine production, ~800 pg/ml). At variance with this finding, the synergistic secretion of IL-1β induced by the EM of the Gram-positive bacterium *S. epidermidis* was only moderately stronger (NP concentration threshold, <25 μg/ml; maximal level of cytokine production, ~3,300 pg/ml) than that induced by the *S. aureus* EM (NP concentration threshold, ~50 μg/ml; maximal level of cytokine production, ~3,200 pg/ml) and comparable to that induced by the *E. coli* EM (Fig. 2C and D). Overall, the synergy between bacterial EMs and SiO_2 NPs in inducing IL-1β in DCs was in the same range as that for SiO_2 NPs and the most effective doses of *E. coli* LPS, which was used here as a positive control, although in this case the threshold concentration of NP was about 100 μg/ml (Fig. 2E). When the dose-response curves of IL-1β secretion and cytotoxicity were compared (see Fig. 1 and the schematic annotation in Fig. 2 showing the range of NP doses corresponding to IC_{50}s), we found interesting differences that were bacterium specific. In fact, in the case of the pathogenic species *P. aeruginosa* and *S. aureus*, IL-1β production occurred only at NP doses well above those inducing strong cytotoxic effects. On the contrary, in the cases of

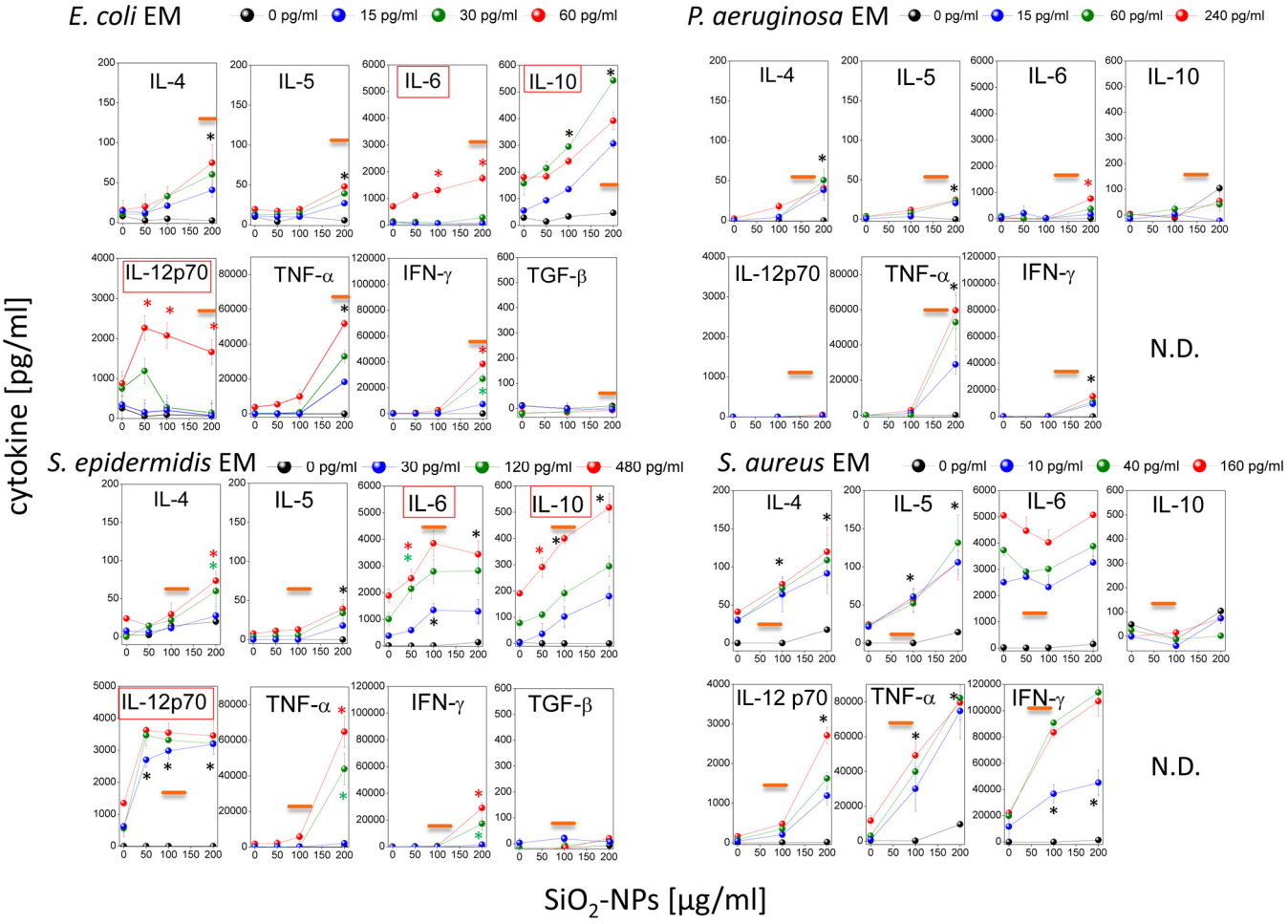

FIG 3 Expression profile of cytokines induced by coincubation of DCs with SiO_2 NPs and bacterium-derived EMs. The extracellular media from DCs that had been treated for 24 h with SiO_2 NPs and EMs, as indicated, were collected, and the concentrations of the indicated cytokines were measured by ELISAs. Data are the means ± SEs ($n = 4$, performed in triplicate). Black asterisks, $P < 0.05$ with respect to cells treated with NPs alone for all EM concentrations used; green or red asterisks, $P < 0.05$ with respect to cells treated with NPs alone for the indicated concentration of EMs (indicated by the green and red symbols, respectively). N.D., not determined. Orange straight lines, IC_{50} values; red boxes, the induction of cytokine release occurred at concentrations less than the IC_{50} values.

commensal *E. coli* and *S. epidermidis* bacteria, significant cytokine secretion was already observed at NP doses with few cytotoxic effects.

Reverse transcription-PCR indicated that EM and NP costimulation improved the transcription of the pre-IL-1β gene (Fig. S3). This suggests that SiO_2 NPs and EMs could also synergize the production of other cytokines (Fig. 3). Indeed, we found that *S. epidermidis* and *E. coli* EMs and SiO_2 NPs synergized IL-12p70, IL-10, and IL-6 (in order of efficacy) production at noncytotoxic NP doses, while they synergized TNF-α, IFN-γ, IL-4, and IL-5 (in order of inefficacy) production only at cytotoxic ones. Notably, the synergistic induction of IL-12p70 and IL-6 production by the *S. epidermidis* EM and SiO_2 NPs was significantly more effective than that by the *E. coli* EM and SiO_2 NPs, while the release of IL-10, TNF-α, IFN-γ, IL-4, and IL-5 showed similar dose-response curves with both EMs. In line with the level of IL-1β secretion, neither the *P. aeruginosa* EM nor the *S. aureus* EM synergized with nontoxic NP doses in inducing the production of any cytokine. However, at toxic NP doses, the *S. aureus* EM was especially effective in synergistically increasing the levels of IL-12p70, TNF-α, and IFN-γ release by DCs and also induced IL-4 and IL-5 release. The *P. aeruginosa* EM induced the weakest synergistic cytokine release by DCs, with the exception of TNF-α induction, the level of which was comparable to that induced by *E. coli* and *S. epidermidis* EMs. The above-documented synergy of SiO_2 NPs and bacterial EMs in inducing the production of IL-1β and other

cytokines was specific for dendritic cells. In fact, in agreement with previous observations (51), in monocytes SiO_2 NPs alone were sufficient to induce IL-1β and TNF-α above a concentration threshold (100 μg/ml), and EMs weakly modulated or did not modulate such effects (Fig. S4).

SiO_2 NPs partially increase the intrinsic ability of *E. coli* and *S. epidermidis* EMs to induce major maturation markers in DCs. We documented above how secreted bacterial factors and SiO_2 NPs synergistically stimulate cytotoxic effects in DCs and the secretion of several cytokines by these cells. Therefore, we also decided to quantify the expression of maturation markers necessary for antigen presentation and T lymphocyte activation (CD86, CD80, CD83, intercellular adhesion molecule 1 [ICAM-1], MHC-II, and MHC-I) on the surface of DCs costimulated with NPs and bacterial EMs (Fig. 4A and B). While SiO_2 NPs alone only marginally increased the basal levels of these markers in DCs, bacterial EMs, as expected, had an intrinsic ability to increase their expression. However, noncytotoxic NP doses further up-modulated the induction of CD80, ICAM-1, MHC-II, CD86, and CD83 (in order of efficacy) by the *E. coli* EM (Fig. 4A). The *S. epidermidis* EM (Fig. 4B) alone had more pronounced intrinsic activity than the *E. coli* EM in the absence of NPs and synergized CD86, ICAM-1, and CD80 expression (in order of efficacy) in the presence of noncytotoxic NP doses. It is to be noted that maturation marker overexpression, even upon NP costimulation, was clearly less than the maximal stimulation, which was induced by the positive control, LPS. In fact, the level of CD86, CD83, and MHC-I induction by *E. coli* EM was suboptimal, weak, and absent, respectively. The *S. epidermidis* EM also induced low levels of CD80, CD83, and MHC-II and did not increase the level of MHC-I expression. Eventually, the effects of the *S. aureus* and *P. aeruginosa* EMs on CD86 and CD83 expression in the presence of NPs were much reduced and absent, respectively, compared to those determined by *E. coli* and *S. epidermidis* EMs (Fig. S5A).

SiO_2 NPs and *E. coli* and *S. epidermidis* EMs synergistically induce DC-mediated T lymphocyte activation. A mixed lymphocyte reaction (MLR) with allogeneic T lymphocytes was performed to assess the immune competence of DCs (Fig. 5). SiO_2 NPs were inactive, while the *E. coli* or *S. epidermidis* EM triggered some T lymphocyte proliferation. However, DCs costimulated with both NPs and bacterial EMs further up-modulated T lymphocyte proliferation, consistent with their synergistic induction of T cell costimulatory molecules. T cell proliferation mediated by DCs pretreated with SiO_2 NPs and the *S. epidermidis* EM reached a maximum at NP doses of about 50 μg/ml and gradually decreased at higher NP concentrations. The synergistic effect of the *E. coli* EM with SiO_2 NPs was smaller than that of *S. epidermidis* EM and SiO_2 NPs, reaching a maximum at NP doses of 150 to 200 μg/ml.

The maximal percentage of T cells induced to proliferate in the MLR assays by DCs stimulated with *E. coli* and *S. epidermidis* in the presence of SiO_2 NPs, obtained at NP doses of 150 μg/ml and 50 μg/ml, respectively, was relatively low (6 to 7%) compared to the percentage induced by optimal LPS doses (22 to 25%) (Fig. S6) and tended to further decrease at higher NP doses, roughly inversely correlating with the intensity of the cytotoxic effects. This may have been due to the only partial onset of DC maturation marker upregulation compared to that achieved with LPS, as mentioned above (Fig. 4). In addition, cytotoxic effects can also explain the reduced level of T cell activation. Indeed, a parallel FACS analysis (Fig. 6A, S7, and S8) indicated the synergistic induction of DC populations by *E. coli* and *S. epidermidis* EMs and high NP concentrations (150 to 200 μg/ml), characterized by reduced side and forward scatter and a lack of CD86 expression. The percentage of these nonresponding DCs (60 to 70%) (Fig. 6B) was even higher than the percentage of DCs showing sign of necrosis (5%) and apoptosis (22%) (Fig. 1C), suggesting that immunocompetent DCs were progressively replaced by dead cells but also by nonfunctional, although still alive, cells unable to undergo immune maturation upon an increase in the NP dose (Fig. 6C).

In spite of this reduced lymphocyte proliferation, we could characterize the main differentiation phenotypes characterizing the activated T cell populations and the cytokines which were released by them. The T lymphocytes induced by DCs treated

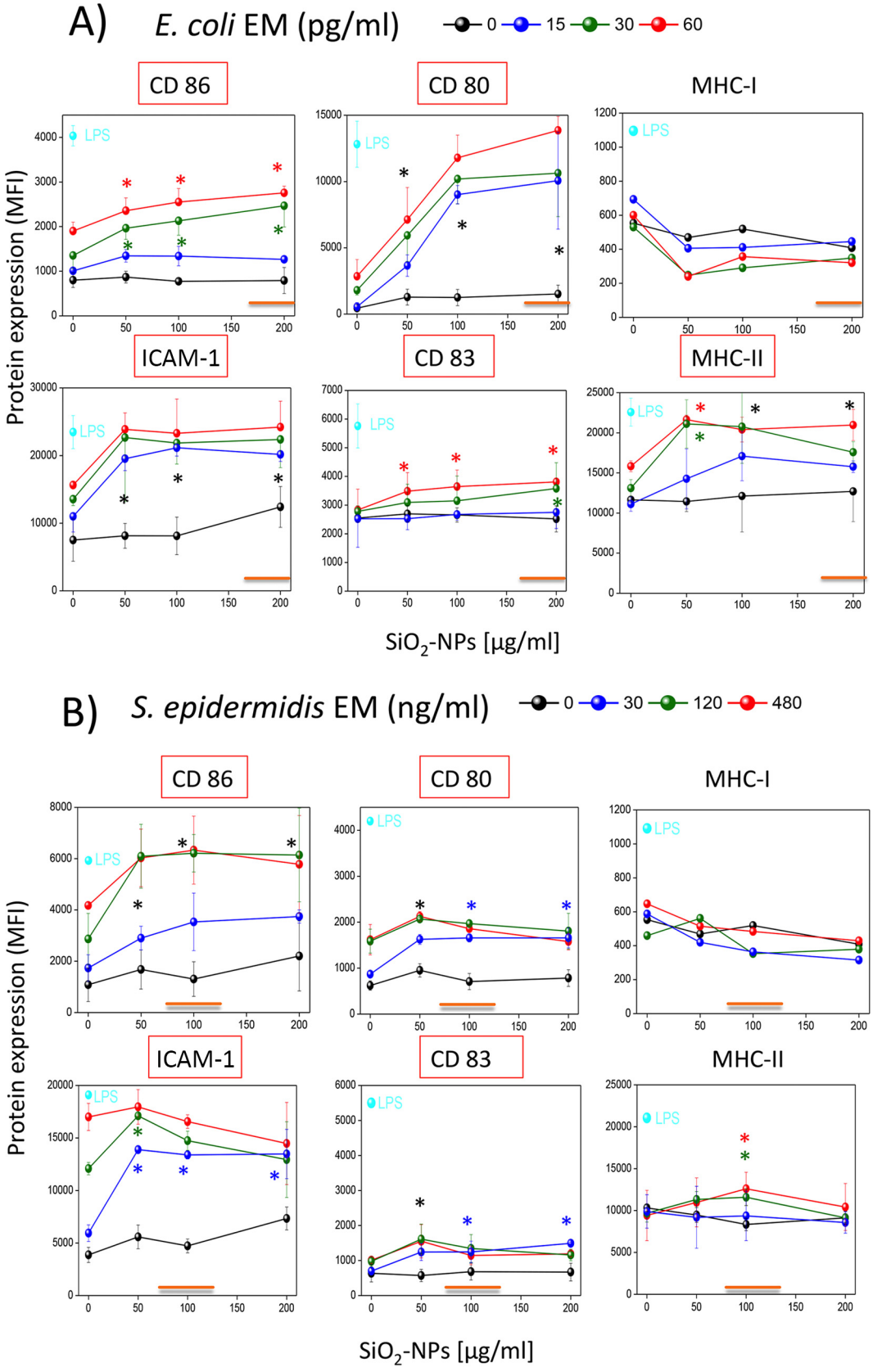

FIG 4 Modulation of the expression of activation markers on DCs coincubated with SiO_2 NPs and bacterium-derived EMs. DCs were incubated for 24 h with SiO_2 NPs alone or in the presence of *E. coli* EM (A) or *S. epidermidis* EM (B) or with *E. coli* LPS as a positive control, as indicated. Cells were then stained with fluorescent antibodies, washed, and analyzed by flow cytofluo-

(Continued on next page)

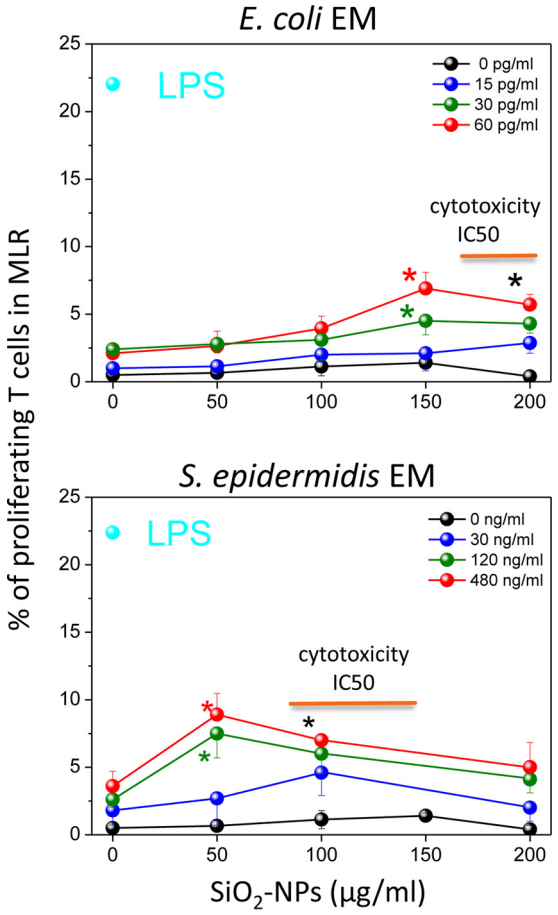

FIG 5 Mixed lymphocyte reaction (MLR) between allogeneic T lymphocytes and DCs pretreated with SiO_2 NPs and bacterial EMs. Allogeneic T cells, prelabeled with CFSE, were incubated for 5 days with DCs that had been preincubated with the indicated doses of SiO_2 NPs and EMs for 24 h and washed before the assay. The percentages of proliferating T cells, identified on the basis of their reduced MFI by FACS, are the means ± SEs ($n = 7$, run in triplicate); the concentration of LPS, which was used as a positive control, was 100 ng/ml. Black asterisks, $P < 0.05$ with respect to cells treated with NPs alone for all EM concentrations used; green or red asterisks, $P < 0.05$ with respect to cells treated with NPs alone for the indicated concentration of EMs (indicated by the green and red symbols, respectively). Orange straight lines, IC_{50} values.

with a low dose of *E. coli* EM (15 pg/ml) and NPs were prevalently $CD4^+$ cells (92% ± 2%). At variance with this finding, in all other situations (DC preincubation with higher *E. coli* EM concentrations, with any *S. epidermidis* EM dose, and with EM plus SiO_2 NPs) the compositions of the activated and proliferating T lymphocytes were rebalanced toward $CD8^+$ cells (~ 60% $CD4^+$ cells and ~40% $CD8^+$ cells) (Fig. 7A). The pattern of cytokine production by these T lymphocytes (Fig. 7B) was prevalently characterized by the proinflammatory cytokines IFN-γ (indicating the likely presence of both $CD4^+$ Th1 and $CD8^+$ Tc1 lymphocyte differentiation) and IL-17A (Th17). In agreement with the MLR dose-response trend (Fig. 5), the level of production of IFN-γ was higher with *S. epidermidis* EM and NP costimulation than with *E. coli* EM and NP costimulation and reached a maximum at 50 to 100 μg/ml NP in the case of NP and *S. epidermidis* EM costimulation. Significant amounts of IL-4 (suggesting Th2 phenotype differentiation)

FIG 4 Legend (Continued)
rimetry. Data are the means ± SEs ($n = 3$, run in triplicate). Black asterisks, $P < 0.05$ with respect to cells treated with NPs alone for all EM concentrations used; green, red, or blue asterisks, $P < 0.05$ with respect to cells treated with NPs alone for the indicated concentration of EMs (indicated by the green, red, and blue symbols, respectively). Orange straight lines, IC_{50} values; red boxes, the induction of marker expression occurred at concentrations less than the IC_{50} values.

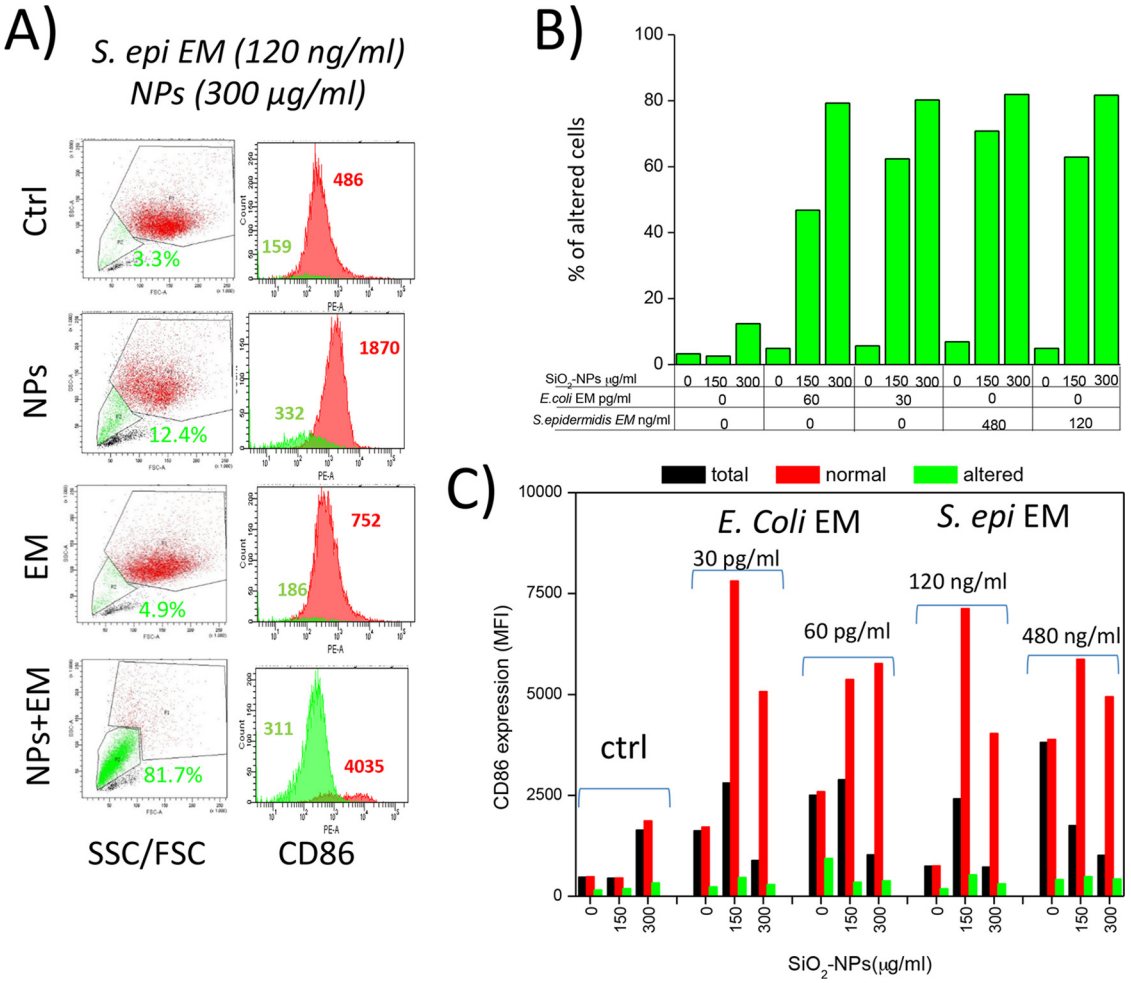

FIG 6 Synergic induction of a DC population unable to overexpress CD86 by SiO_2 NPs and bacterial EMs. (A) Illustrative dot plots and histogram plots of CD86 expression distributions obtained by FACS analysis of DCs treated for 24 h with SiO_2 NPs and EMs. Gating, the percentage of anomalous cells (green) with reduced side and forward scattering properties, and their corresponding levels of CD86 expression (indicated as MFI values) are shown. Red histogram plots represent functional DCs with forward scatter (FSC) and side scatter (SSC) parameters similar to those of control (Ctrl) cells; green histogram plots represent anomalous dendritic cells that had forward scatter and side scatter parameter values lower than those of control cells and that were unable to undergo maturation. Data are from 1 representative experiment of 10 experiments conducted. (B) Illustrative histogram plots of the CD86 MFI expressed by dendritic cells after 24 h of incubation with the different stimuli indicated in the figure. Numbers indicate the MFI of the peak. Data represent the percentage of altered DCs (with low forward scatter and side scatter parameter values) after treatment with different NP and EM concentrations. (C) CD86 expression (indicated as MFI values) by total cells (with no gating in dot plots), normal cells (gated by means of their forward scatter and side scatter values similar to those for control cells), and shrunken cells (gated by means of their low forward scatter and side scatter values) after DC treatment (with NPs alone or with different concentrations of EMs). *S. epi*, *S. epidermidis*.

and of IL-6 were also induced by *S. epidermidis* EM and NP cotreatment but not by *E. coli* EM and NP cotreatment. The levels of IL-5 induced by *E. coli* and *S. epidermidis* EM alone were not increased significantly by NP costimulation; on the contrary, there was a significant inhibitory effect due to NP costimulation. The anti-inflammatory cytokines IL-10 and transforming growth factor β (TGF-β) were not significantly induced in either case. The *S. aureus* EM did not induce a significant increase in the amount of lymphocyte-derived cytokines, in agreement with the lack of a synergistic effect of the *S. aureus* EM and NPs in increasing DC-mediated T cell activation (Fig. S9).

Role of protein bacterial factors and of their nanoparticle adsorption in synergy of EMs and SiO_2 NPs. SiO_2 NPs are captured by DCs at the physiologic temperature (37°C), while they are not captured at 0°C, a fact suggesting their active internalization (Fig. S10). Therefore, it is possible that bacterial EMs exert their synergy with NPs, resulting in cytotoxic, proinflammatory, and proimmune effects in DCs, by increas-

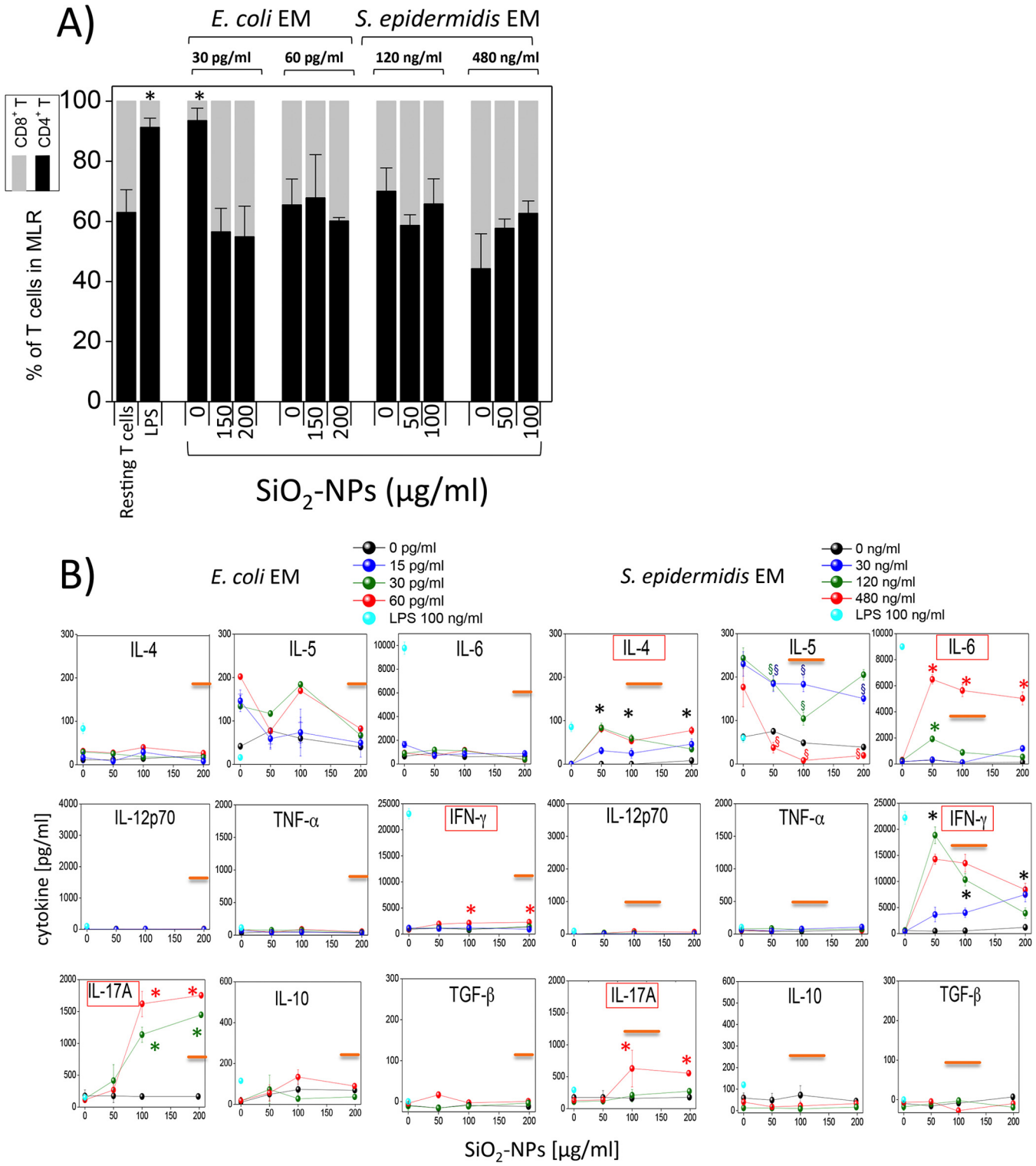

FIG 7 Percentages of $CD4^+$ and $CD8^+$ cells and cytokine release by allogeneic T lymphocytes mixed with DCs pretreated with SiO_2 NPs and bacterial EMs. (A) The relative amounts of $CD4^+$ T cells and $CD8^+$ T cells among resting or DC-induced proliferating lymphocytes after preincubation with LPS or NPs and EMs were determined by FACS analysis using specific antibodies (means ± SEs; $n = 4$, run in triplicate). *, $P < 0.05$ with respect to control cells. (B) Relative amounts of cytokines produced by allogeneic T lymphocytes after 5 days of incubation with DCs preincubated for 24 h with SiO_2 NPs and bacterial EMs, as indicated. Data are from one representative experiment of four experiments conducted and represent means ± SEs. Black asterisks, $P < 0.05$ with respect to cells treated with NPs alone for all the EM concentrations used; green or red asterisks, $P < 0.05$ with respect to cells treated with NPs alone for the indicated concentration of EMs (indicated by the green and red symbols, respectively); green, blue, or red section signs, $P < 0.05$ with respect to cells treated with NPs alone for the indicated concentration of EMs (indicated by the green, blue, and red symbols, respectively). Orange straight lines, IC_{50} values; red boxes, induction of cytokine release occurred at concentrations less than the IC_{50} values.

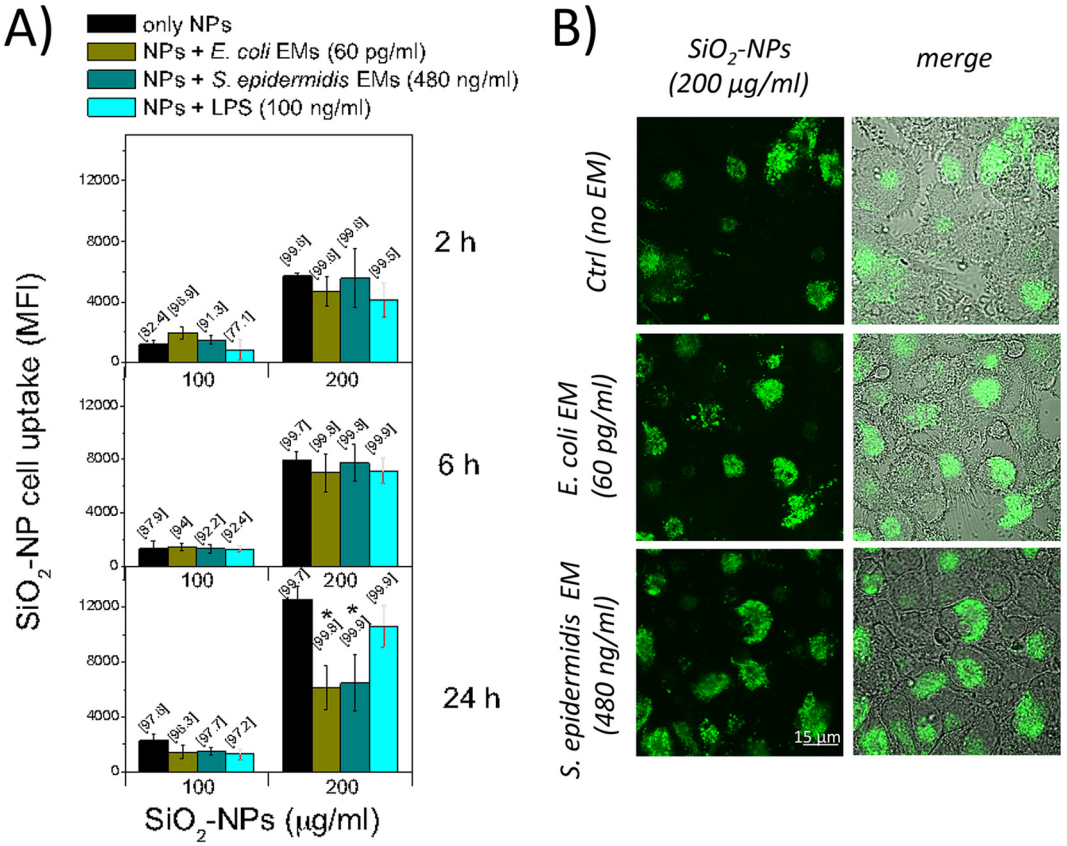

FIG 8 SiO_2 NP uptake by DCs is not affected by the presence of bacterial EMs. (A) After incubation at 37°C with FITC-labeled Stöber SiO_2 NPs, bacterial EMs, or *E. coli* LPS as a positive control, NP uptake by DCs was quantified by flow cytofluorimetry. Data, expressed as MFI, are means ± SEs ($n = 2$, run in duplicate). The percentage of positive cells is indicated in brackets. *, $P < 0.05$ with respect to samples treated with NPs alone. (B) DCs were placed on poly-L-lysine-coated slides and left untreated in the heated chamber for 5 min to allow adhesion to the surface of the slides; then, the cells were incubated with FITC-labeled Stöber NPs and bacterial EMs, as indicated, for 2 h, washed, and directly analyzed by confocal microscopy.

ing the efficacy with which they capture NPs. We tested this possibility for *E. coli* and *S. epidermidis* EMs, which showed the best synergic actions even at noncytotoxic NP doses. The results, however, showed no increase in the level of NP binding (Fig. 8A) or internalization (Fig. 8B) by DCs costimulated with EMs compared to that by control DCs during the first 6 h and partial inhibition after 24 h, compatible with a cytotoxic phenomenon.

Then, to increase our understanding of the nature of the bacterial factors involved in synergy, we pretreated EMs with proteinase K to digest proteins and tested the ability of the EMs obtained to synergize with NPs to upregulate CD86 and induce IL-1β production. The results showed that the maturation marker upregulation induced by *E. coli* and *S. epidermidis* EMs after proteinase K digestion in the presence of SiO_2 NPs was not affected, suggesting that nonprotein agonists are responsible for this effect (Fig. 9A, top). At variance with this finding, IL-1β secretion under the same conditions was strongly dependent on a proteinase K-sensitive protein factor in the case of *E. coli*, while it was largely independent of protein factors in the case of *S. epidermidis* (Fig. 9A, bottom). These data indicate that the induction of cytokines and the upregulation of CD maturation markers are synergized by different sets of bacterial agonists in *E. coli* and that nonproteinaceous pathogen-associated molecular pattern (PAMPs) are mostly responsible for the synergic action of *S. epidermidis*. On the contrary, proteinaceous factors are mostly responsible for the synergistic activity of *E. coli* and NPs for IL-1β induction.

Eventually, since SiO_2 NPs can bind proteins with a high affinity (36), we assessed the possibility that the observed synergic effects were due to the physical association of

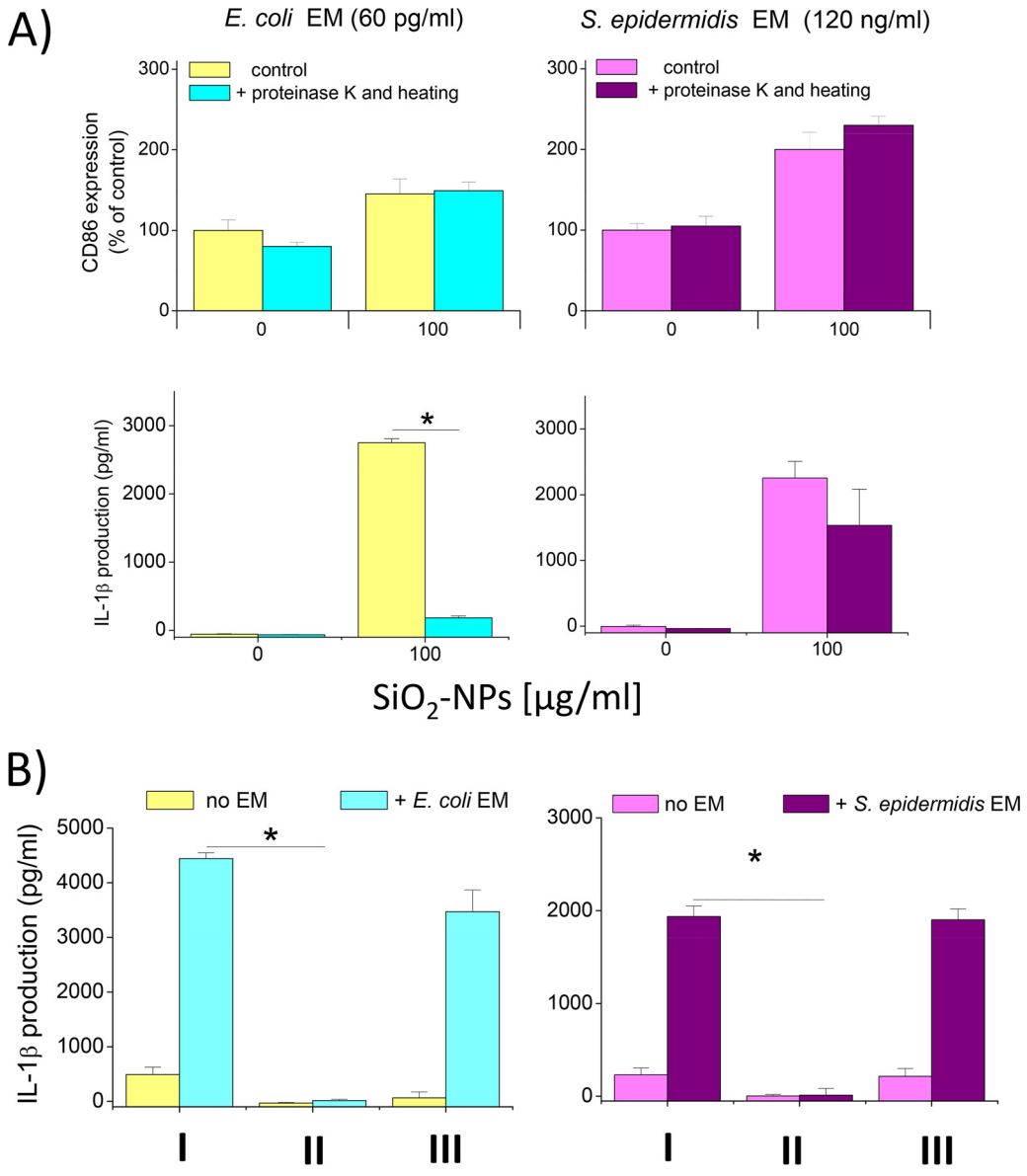

FIG 9 Dependence of NP and EM synergy on proteinaceous PAMPs and on an association with bacterial factors on the surface of NPs. (A) DCs were treated (for 24 h at 37°C) with EMs or with EMs that had been incubated for 1 h at 50°C with 100 μg/ml proteinase K and then for 5 min at 95°C in order to degrade proteins; the cells were then analyzed for CD86 expression (top), and the amount of IL-1β in the culture supernatant was measured (bottom); data are from one representative experiment of three experiments conducted and represent means ± SEs. *, $P < 0.05$ with respect to cells not treated with proteinase K. (B) NPs (100 μg/ml) were incubated with the indicated EM concentrations for 20 min at 37°C in RPMI 1640 containing 10% FBS. The NPs were then centrifuged for 30 min at 13,000 rpm, and the supernatant was recovered. The NPs were washed three times with PBS, and finally, some NPs were resuspended in fresh medium and other NPs were resuspended with the recovered supernatant. Then, the NPs were used to treat DCs for 24 h at 37°C and IL-1β production was measured by ELISA. Data are from one representative experiment of three experiments conducted and represent means ± SEs. *, $P < 0.05$. I, NPs coincubated with the indicated medium and DCs; II, NPs preincubated with the indicated medium, pelleted, and incubated with DCs after resuspension in new medium without EM; III, NPs preincubated with the indicated medium, pelleted, and incubated with DCs after resuspension in their corresponding supernatants.

bacterial factors with NPs, a fact that could favor the targeting of a bound bacterial agonist(s) thanks to its effective binding and endocytosis by DCs. To test this hypothesis, NPs preincubated with EMs from *E. coli* and *S. epidermidis* were centrifuged and washed to eliminate unbound proteins and used to stimulate DCs in the presence of fresh medium free of EM. The data show that the washed NPs decorated with the protein corona obtained after incubation with both *E. coli* and *S. epidermidis* lost their ability to trigger IL-1β secretion (Fig. 9B). However, when the supernatant still contain-

ing the EM was coincubated with washed NPs, the synergy was fully restored. These data demonstrate that the bacterial factor(s) responsible for the synergic effects on DC activation shown here did not act after adsorption on NPs to become a part of their corona but acted as a free agonist in solution able to costimulate DCs independently.

DISCUSSION

Our study stemmed from the consideration that DCs are major controllers of the inflammatory balance and of the immune defenses in both mucosae and skin and continuously monitor signals derived from the commensal bacteria present there. In addition, NPs, present as additives or excipients in several foods, drugs, and cosmetics, are likely to be normally ingested by humans or to come into contact with their skin. Hence, we asked if the costimulation of DCs with NPs and bacterially secreted molecules could substantially influence the responses of these cells. To achieve this aim, we used amorphous silica nanomaterial in the form of nanoparticles (SiO_2 NPs), due to their widespread use in food and pharmaceutical products, and mixtures of factors spontaneously released under culture conditions by two common commensals, a Gram-negative bacterium, *E. coli*, which is present in the gut, and a Gram-positive bacterium, *S. epidermidis*, which is present on the skin. For comparison, we also used similar preparations from common Gram-negative and Gram-positive bacteria that act as opportunists/pathogens (*P. aeruginosa* and *S. aureus*, respectively).

A major result of our study is that all bacterial factors tested increased the cytotoxic effects and the levels of cytokine production in DCs contemporaneously engaged in SiO_2 NP capture, while only those factors derived from commensal species also stimulated their immune maturation. Moreover, as summarized in Table 1, the pattern of induction of cytokines and the pattern of the proimmune effects not only had distinctive traits according to the type of bacterial costimulus but also differently correlated with cytotoxic phenomena. At NP doses determining weak cytotoxicity, the synthesis of major cytokines regulating inflammation and T lymphocyte differentiation, like IL-1β, IL-12, IL-10, and IL-6, was synergized only by a commensal *E. coli* or *S. epidermidis* costimulus. Interestingly, some of the cytokines are proinflammatory (IL-1β and IL-12), while some are anti-inflammatory (IL-10 and IL-6), suggesting the synergic induction of counteracting signals. However, at cytotoxic NP doses, we extended the set of cytokines induced by costimulation with commensal bacteria to TNF-α, IFN-γ, IL-4, and IL-5 and also detected the emergence of cytokine release by costimulation with pathogenic bacteria (IL-12, TNF-α, IFN-γ, IL-6, IL-4, IL-5). Similarly, although the upregulation of maturation markers was not complete and had distinctive attributes, depending on the bacterial species (CD80, CD86, CD83, ICAM-1, and MHC-II in the case of *E. coli* and CD80, CD86, and ICAM-1 in the case of *S. epidermidis*), the increased ability to support T lymphocyte activation was consistently induced only by commensal bacterial factors and was more effective with poorly cytotoxic NP concentrations. T lymphocyte activation by DCs is a crucial factor since it is expected to amplify inflammatory signals and effects. In fact, the pattern of cytokine secretion by activated DCs, which was characterized by the prevalence of IL-12, and DC-induced T lymphocyte cytokines, which were mostly IFN-γ and IL-17A, together with major differentiation marker analysis, suggested the preferential tendency of DCs to trigger a $CD4^+$ Th1/$CD8^+$ Tc1 response in the presence of NPs and *S. epidermidis*- and *E. coli*-derived factors. Such T lymphocytes are proinflammatory, due to their ability to produce IFN-γ, a major cytokine able to improve macrophage activities, and IL-17A, a cytokine activating the recruitment of PMNs.

Still, it is important to stress how the NP dose can affect the above-described amplification of the inflammatory action mediated by activated T lymphocytes. In fact, when cytotoxicity increased at higher NP doses, the levels of lymphocyte proliferation and cytokine secretion decreased, presumably due to the prevalence of adverse reactions over the immune maturation of cells, as shown by the progressive appearance of cells unable to upregulate CD86. Once again, in the case of a costimulus with

TABLE 1 Summary of synergistic activity of EMs and SiO_2 NPs on DCs[a]

		cytotoxic effect on DCs according to SiO_2- NPs dose					
		+	++	+	++	+	++
	EM	DC cytokines		DC maturation markers		T Lymphocyte activation	
commensals	*E. coli*	IL-1-β; IL-12p70 IL-6; IL-10	IL-1β; IL-12p70; IL-6; IL-10 TNFα; IFNγ IL-4; IL-5	ICAM-1 CD80 CD86 MHC-II CD83	ICAM-1 CD80 CD86 MHC-II CD83	• proliferation: +/- • diff markers: CD 4 and CD8 • Cytokines: IL-17A, IFNγ	• proliferation: +/- - • diff markers: CD4 and CD8 • Cytokines: IL-17A, IFNγ
	S. epidermidis	IL1-β; IL-12p70 IL-6; IL-10	IL1-β; IL-12p70 IL-6; IL-10 TNFα; IFNγ IL-4; IL-5	CD86 ICAM-1 CD80 CD83	CD86 ICAM-1 CD80 MHC-II CD83	• proliferation: + • diff markers: CD 4 and CD8 • Cytokines: IL-6, IFNγ, IL-4	• proliferation: +/- • diff markers: CD 4 and CD8 • Cytokines:I L-6, IFNγ, IL-4, IL17A
pathogens	*P. aeruginosa*	no	IL1-β; IL-6; TNFα IFNγ; IL-4; IL-5	no	CD86	• proliferation: n.d.	• proliferation: n.d.
	S. aureus	no	IL1-β; IL-12 TNFα; IFNγ IL-4; IL-5	no	CD86	• proliferation: n.d.	• proliferation: n.d.

[a]The increase in the levels of cytokine production and maturation marker induction by DCs and the T lymphocyte-activating capacity (proliferation, phenotype differentiation [diff], and cytokine secretion) due to EM and NP costimulation were correlated with cytotoxic phenomena. Changes occurring at cytotoxic NP doses are highlighted in red. The following semiquantitative notations are used to help the reader recall the rough intensity of the parameters analyzed: +/−−, very weak effect; +/−, weak effect; +, an effect; ++, a strong effect; ND, not determined.

pathogenic bacteria, no maturation marker expression or T lymphocyte activation was observed at any NP dose.

In short, we conclude that SiO_2 NPs at subtoxic doses and the molecules released by commensal microbes (*S. epidermidis* and *E. coli*) synergistically stimulate DCs (more effectively by *S. epidermidis* than by *E. coli*) to release several proinflammatory, anti-inflammatory, and regulatory cytokines and to mature into immunocompetent cells potentially able to trigger the proliferation of both $CD4^+$ and $CD8^+$ T lymphocytes, which in turn are able to amplify the proinflammatory signals in the presence of antigens. At variance with this finding, *S. aureus* and *P. aeruginosa* factors are defective in synergizing DC immune maturation and synergize their direct production of inflammatory cytokines only in the presence of SiO_2 NP concentrations leading to strong cytotoxic effects.

It is interesting to note that while the upregulation of maturation markers by *E. coli* and *S. epidermidis* and of IL-1β secretion by *S. epidermidis* was largely mediated by nonprotein molecules, the full synergic induction of cytokines, on the contrary, required protein factors from *E. coli*. We also showed that the effects of these nonprotein or protein agonists do not depend on their strong binding to SiO_2 NPs as part of the nanoparticle serum corona but are due to their independent agonistic action on DCs.

The enhancing effect of factors of commensal bacteria on DC-mediated inflammatory reactions in the presence of amorphous SiO_2 NPs is an interesting and new observation, since it has been shown, on the contrary, that the activation of lung- or bone marrow-derived murine DCs mediated by Toll-like receptor agonists is suppressed in the presence of crystalline SiO_2 particulates (52).

Moreover, a general message from our data is that DCs, which are potentially able to unleash compounds that produce harsh inflammation and immune reactions, may be a hot spot in nanotoxicology. In fact, our amorphous model of SiO_2 NPs, tested here because of the likely exposure of humans to additives based on this material as well as,

possibly, other NPs, might accentuate the response of DCs to commensal microbes, thus exacerbating not only adverse inflammatory effects but also the specific immune reaction to other antigens entering the tissue. For example, the enhanced tendency of *S. epidermidis*- and *E. coli*-derived compounds to favor IFN-γ production in the presence of nanoparticles might increase the risk of allergic and immune-mediated inflammation, like DTH reactions, in subjects exposed to these nanomaterials or worsen the symptoms in individuals already presenting these pathologies. This does not exclude the possibility that other myeloid antigen-presenting cells (monocytes and macrophages) or non-antigen-presenting cells, such as leukocytes (e.g., polymorphonuclear neutrophil granulocytes [PMNGs]), could also be subjected to synergic effects upon stimulation with NPs and microbes. It has been demonstrated that amorphous silica nanoparticles are endocytosed by macrophages (51) and that incubation with increasing amounts of silica NPs increased the percentages of dead cells and the parallel induction of proinflammatory cytokine IL-1β release. In fact, formyl peptide receptor agonists have been shown to synergize cytokine production by monocytes and the chemotactic response in PMNGs in the presence of SiO_2 NPs. However, no upregulation of maturation markers like that which was shown to occur in DCs was induced in these cells (39). No data on the possible up-modulation of costimulatory markers in macrophages under the conditions used in this study are currently available. Given that macrophages are also important drivers of inflammation and have antigen presentation roles, future investigations to elucidate their possible role together with DCs in the scenario that we depict are required to fill this gap.

Our *in vitro* study indicates that the host microbiome may be a constitutive factor in determining the bioactivity and biocompatibility of NPs by altering the regulatory role of DCs. In this scenario, not only the chemical nature and dose of nanoparticles but also the type and virulence of modulatory microbial factors become critical variables and should be considered when the toxicity and safety of NPs are assessed. The possible interactions between nanosystems and the resident microbial flora may be even more complex than what can be inferred from our data, which were obtained using factors for single bacterial species, since several factors from different commensal bacterial species could act in a synergistic or an additive way. Therefore, *in vivo* data are crucial to establish if these data are significant. This implies that future efforts should concentrate on the task of developing appropriate animal models, especially for application to cosmetic and food products, amenable to manipulation of a microbiome resembling the one present in humans. On the other hand, our results justify a comprehensive characterization of the *E. coli* and *S. epidermidis* secretome joined with biochemical and functional analysis to identify those specific protein and nonprotein factors involved in the regulation of DCs and possibly other immune cells present in human tissues potentially exposed to nanoparticulates.

MATERIALS AND METHODS

NP synthesis and characterization. Ludox TM-40 amorphous silica nanoparticles (40% [wt/vol] in H_2O) were from Sigma-Aldrich. Dynamic light scattering (DLS) indicated that these nanoparticles had an average diameter of 28 nm and a polydispersity index (PDI) (in phosphate-buffered saline [PBS], pH 7.4) of 0.205. The zeta potential was −13.7 mV. TEM analysis yielded a diameter of 27 nm. NPs were endotoxin free (<0.05 endotoxin unit/ml, as measured by the *Limulus* amoebocyte lysate test). Fluorescein isothiocyanate (FITC)-labeled Stöber SiO_2 NPs, prepared as described previously (51), had a mean diameter of 30 nm and a PDI (in phosphate-buffered saline [PBS]), pH 7.4 of 0.198 by DLS and a diameter 24 nm by TEM, while the zeta potential was −18.8 mV.

Bacterial cultures and preparation of cell-free extracellular media from cultures. *Escherichia coli* ATCC 25922 (serotype O6, biotype 1), *Pseudomonas aeruginosa* (ATCC 25668; strain designation, NCTC 10662), methicillin-resistant *Staphylococcus aureus* strain ATCC BAA-44 (strain designation, HPV107), and *Staphylococcus epidermidis* ATCC 700565 (strain designation, 4477-2) were precultured in 5 ml LB broth at 37°C for 2 h. The cultures were transferred to 100 ml LB broth and further grown overnight at 37°C. Bacteria were collected, and the optical density at 620 nm was measured. Then, after centrifugation at 6,000 × *g* for 15 min at 4°C, the extracellular media (EM) were filtered (pore size, 0.25 μm). The EM protein concentration was estimated by the Bradford assay (Bio-Rad). LPS from *Escherichia coli* serotype O26:B6 was from Sigma-Aldrich. In some experiments, EMs, concentrated 10-fold with respect to the final concentrations in cellular assays, were pretreated with 100 μg/ml proteinase K (Promega) for 60 min at

50°C, incubated at 95°C for 5 min, diluted 10-fold in culture medium, and used to treat dendritic cells (DCs) as indicated below.

DC production. Blood samples derived from healthy donors were kindly provided by the transfusion center of the Hospital of Padua. Blood leukocytes were not obtained for experimentation on humans but as a consequence of voluntary and informed blood donation for transfusions. No approval of an ethics committee is needed in such cases in our institution. Peripheral blood mononuclear cells (PBMCs) were isolated from buffy coats by sequential Ficoll-Hypaque and Percoll density gradient centrifugations (GE Healthcare). PBMCs in RPMI 1640 (Gibco) plus 2% fetal bovine serum (FBS; EuroClone) and antibiotics (100 U/ml penicillin and 100 μg/ml streptomycin; Invitrogen) were plated onto a 24-well plate (Falcon) at a density of 2×10^6 cells/well. After 1 h, residual lymphocytes were removed and monocytes were cultured at 37°C in a humidified atmosphere containing 5% (vol/vol) CO_2 in RPMI 1640 with 10% FBS. Human immature DCs were differentiated from monocytes isolated with RosetteSep monocyte enrichment cocktail (StemCell Technologies). Monocytes (10×10^6/ml) in RPMI 1640 with 2% FBS were allowed to adhere to 6-well plates (Corning), and after 1 h at 37°C, nonadherent cells were removed and the remaining cells were cultured for 5 days in RPMI 1640 with 10% FBS supplemented with 50 ng/ml granulocyte-macrophage colony-stimulating factor and 20 ng/ml IL-4 (Miltenyi Biotec). The medium was refreshed on day 4. After day 5, cells were collected, plated onto a 48-well tray (2×10^6 cells/well; Corning), and stimulated with the various stimuli. Human lymphocytes were purified from the buffy coat with the RosetteSep human T cell enrichment cocktail (StemCell Technologies) according to the manufacturer's protocol and cultured in RPMI 1640 with 10% FBS at 37°C in 5% (vol/vol) CO_2.

Cytotoxicity assays. DCs plated in 96-well trays (5×10^4/well) were incubated in RPMI 1640 with 10% FBS for 24 h at 37°C with SiO_2 NPs (up to 300 μg/ml) with or without bacterial EMs and subjected to an MTS assay (Promega) according to the guidelines in the instruction manual. The absorbance at 495 nm was quantified by use of a microplate reader (Thermo Fisher Scientific), and cell viability was expressed as a percentage of that for the controls. The IC_{50} (the concentration of NPs at which 50% of the cells died) was calculated for each peptide and each kind of cell tested. For apoptosis/necrosis assays, DCs treated as described above were stained with annexin V according to the manufacturer's instructions (Roche), washed, and suspended in FACS buffer; 15 μl of PI was added to each sample just before acquisition by cytofluorimetry; apoptosis and necrosis were estimated on the basis of annexin V and PI positivity. Data for 10,000 events were collected and analyzed by the use of FACSDiva software (BD).

Cytokine quantification. The release of IL-1β, IL-10, TGF-β, and IFN-γ and of IL-6 and TNF-α in DC supernatants after 24-h treatments was assayed by the use of enzyme-linked immunosorbent assay (ELISA) kits according to the manufacturers' instructions (eBioscience for IL-1β, IL-10, TGF-β, and IFN-γ; Peprotech for IL-6 and TNF-α). The absorbance at 405 nm was quantified with a plate reader (Thermo Fisher Scientific). Cytokine release by activated T cells after mixed lymphocyte reactions (MLRs) was investigated with an ELISA kit (for TGF-β and IL-10; eBioscience) or with a Th1/Th2 cytokine panel (for IFN-γ, IL-6, IL-4, IL-5, IL-12p70, and TNF-α; eBioscience) and analyzed by use of a Bio-Plex system following the manufacturer's protocol. In some experiments, the amounts of cytokines in DCs treated with NPs preincubated with cell culture medium plus FBS in the presence of EMs or without EMs were quantified, in which case the DCs were centrifuged (at 13,000 rpm for 30 min), washed three times with PBS, and subsequently centrifuged as described above to obtain the hard corona-NP complexes. The isolated NPs were incubated with cells with fresh medium plus FBS or with the equivalent medium (with or without EMs) that remained in the supernatant after the NP first centrifugation.

Induction of pro-IL-1β in DCs by NPs and EMs. DCs were incubated at 37°C for 3 h with SiO_2 NPs (100 μg/ml) and different EMs or with LPS (1 μg/ml) as a positive control. Cells were then scraped off, and RNAs were isolated by use of the TRIzol reagent (Invitrogen) according to the manufacturer's instructions and eventually suspended in 10 μl of RNase-free water (Gibco). RNA was quantified by spectrophotometric analysis (NanoDrop ND-1000 spectrophotometer; Celbio), and 300 ng of total RNA was retrotranscribed. First-strand cDNA was prepared by using Moloney murine leukemia virus reverse transcriptase (Promega) with random primers (Promega) and was used for PCR analysis. Equal amounts of cDNA were amplified by PCR with GoTaq Flexi DNA polymerase (Promega) and a reaction buffer containing $MgCl_2$, a PCR nucleotide mix (Promega), and the following primers: for IL-1β, 5′-CTGTCCTGCGTGTTGAAAGA-3′ and 5′-TTGGGTAATTTTTGGGATCTACA-3′, and for GAPDH (glyceraldehyde-3-phosphate dehydrogenase), 5′-AGCAACAGGGTGGTGGAC-3′ and 5′-GTGTGGTGG GGGACTGAG-3′. The PCR program had the following parameters: initial denaturation for 2 min at 94°C, 30 steps of PCR cycling consisting of denaturation for 1 min at 94°C and annealing for 1 min at 57°C and 20 s at 72°C, and a final extension for 5 min at 72°C.

Analysis of DC maturation markers. After 24 h of incubation, DCs were collected, suspended in FACS buffer (1% FBS, 0.1% NaN_3 in PBS), stained with fluorescent mouse anti-human immunoglobulin monoclonal antibodies (CD80-FITC, CD83-phycoerythin [PE]-Cy7, CD86-peridinin chlorophyll protein-Cy5.5, MHC-I–PE, MHC-II–allophycocyanin [APC]-H7, CD54 [ICAM-1]-APC, and CD1a-PE; BioLegend and BD) for 30 min at 4°C in the dark, and analyzed by flow cytofluorimetry (FACSCanto II; BD) using FACSDiva software; data for 10,000 events were collected. Background cell fluorescence values were not significantly changed after incubation with SiO_2 NPs (see the example in Fig. S5B in the supplemental material) and were subtracted from the signals determined by antibody labeling.

MLR and T cell phenotype determination. After a 24-h treatment with SiO_2 NPs (50 to 200 μg/ml) and EMs, DCs were collected and centrifuged at 1,500 rpm for 5 min, and the pellet was irradiated with 4,000 rads of ^{137}Cs gamma radiation to prevent proliferation. The DCs were then suspended in RPMI 1640

plus 10% FBS and seeded in 96-well plates (2×10^5 cells/well; Corning). Allogeneic T cells were isolated from the buffy coat by negative selection using RosetteSep enrichment cocktail. The T cells (10×10^6 cells/ml in PBS) were labeled with 5 μM CellTrace carboxyfluorescein succinimidyl ester (CFSE) probe (Invitrogen) for 5 min at 37°C. They were then washed and suspended in RPMI 1640 plus 10% FBS, and the suspension was added to DCs (2×10^5 DCs, 10^5 T cells/well). The cells were cocultured for 3 to 6 days at 37°C. DC-induced T cell proliferation was measured by flow cytometry with gating for T cells and calculating the percentage of cells with a reduced CFSE mean fluorescence intensity (MFI) by subtraction of background values (range, 3 to 9%). Phytohemagglutinin (PHA; 10 μg/ml; Sigma) was used as a positive control for the assay. In some experiments, cells were collected, labeled with anti-human $CD4^+$/$CD8^+$ antibodies (BioLegend), and analyzed by cytofluorimetry; data for 10,000 events were collected.

SiO_2 NP binding to DCs. The intracellular distribution of FITC-labeled Stöber SiO_2 NPs was assessed by confocal microscopy. DCs (2×10^5) were allowed to adhere to poly-L-lysine (50 μg/ml; Sigma-Aldrich)-precoated glass slides (20 min in RPMI 1640 plus 10% FBS at 37°C), incubated for 24 h at 37°C with NPs alone or in the presence of bacterial EMs, washed with PBS, and directly analyzed by confocal microscopy (Leica SP2). Images were processed using ImageJ software. Alternatively, DCs (2×10^5 cells/well) were incubated with FITC-labeled Stöber SiO_2 NPs alone or in the presence of bacterial EMs for 3 to 24 h at 37°C or 0°C. Cell MFI values were obtained by cytofluorimetry and analyzed by the use of FACSDiva software; data for 10,000 events were collected. The background cell fluorescence was subtracted.

Statistical and mathematical analysis. Cytotoxicity dose-response data were fit nonlinearly with logistic curves, as follows: $y = \{(A_1 - A_2)/[1 + (x/x_0)^p]\} + A_2$, where y is the MTS reduction rate, A_1 is the background toxicity (no NPs), A_2 is the final cytotoxicity (maximum NP cytotoxicity), x is the NP dose, x_0 is the NP dose resulting in half of the maximum effect, and p is power. The 50% effective concentrations (x_0) were deduced from statistically significant convergent curves. The data were checked for a normal (Gaussian) distribution, and this was confirmed by the Shapiro-Wilks test (0.05 level). The significance of the differences between means (0.05 level) was evaluated by a two-sample or paired t test, when applicable, and by analysis of variance.

SUPPLEMENTAL MATERIAL

Supplemental material for this article may be found at https://doi.org/10.1128/CVI.00178-17.

SUPPLEMENTAL FILE 1, PDF file, 0.7 MB.

ACKNOWLEDGMENTS

We thank the Centro Trasfusionale of the Hospital of Padua (ULSS 16) for buffy coats and A. Geffner Smith for editing.

This work was supported by PRIN 2011 and by PRAT 2011 and ex60% 2013-2016 from the University of Padua, Progetto Strategico (NAMECA) from the University of Padua, and FIRB 2011 from the Italian Ministry of Research.

We have no financial conflicts of interest.

REFERENCES

1. Oberdorster G, Oberdorster E, Oberdorster J. 2005. Nanotoxicology: an emerging discipline evolving from studies of ultrafine particles. Environ Health Perspect 113:823–839. https://doi.org/10.1289/ehp.7339.
2. Borm PJ. 2008. Future interactions in particle toxicology: the role of PFT. Part Fibre Toxicol 5:5. https://doi.org/10.1186/1743-8977-5-5.
3. Oberdorster G. 2010. Safety assessment for nanotechnology and nanomedicine: concepts of nanotoxicology. J Intern Med 267:89–105. https://doi.org/10.1111/j.1365-2796.2009.02187.x.
4. Abdel-Mottaleb MM, Try C, Pellequer Y, Lamprecht A. 2014. Nanomedicine strategies for targeting skin inflammation. Nanomedicine (Lond) 9:1727–1743. https://doi.org/10.2217/nnm.14.74.
5. Lamprecht A. 2015. Nanomedicines in gastroenterology and hepatology. Nat Rev Gastroenterol Hepatol 12:195–204. https://doi.org/10.1038/nrgastro.2015.37.
6. Fernandez TD, Pearson JR, Leal MP, Torres MJ, Blanca M, Mayorga C, Le Guevel X. 2015. Intracellular accumulation and immunological properties of fluorescent gold nanoclusters in human dendritic cells. Biomaterials 43:1–12. https://doi.org/10.1016/j.biomaterials.2014.11.045.
7. Herd HL, Bartlett KT, Gustafson JA, McGill LD, Ghandehari H. 2015. Macrophage silica nanoparticle response is phenotypically dependent. Biomaterials 53:574–582. https://doi.org/10.1016/j.biomaterials.2015.02.070.
8. Jimenez-Perianez A, Abos Gracia B, Lopez Relano J, Diez-Rivero CM, Reche PA, Martinez-Naves E, Matveyeva E, Gomez del Moral M. 2013. Mesoporous silicon microparticles enhance MHC class I cross-antigen presentation by human dendritic cells. Clin Dev Immunol 2013:362163.
9. Kang K, Lim JS. 2012. Induction of functional changes of dendritic cells by silica nanoparticles. Immune Netw 12:104–112. https://doi.org/10.4110/in.2012.12.3.104.
10. Kunzmann A, Andersson B, Vogt C, Feliu N, Ye F, Gabrielsson S, Toprak MS, Buerki-Thurnherr T, Laurent S, Vahter M, Krug H, Muhammed M, Scheynius A, Fadeel B. 2011. Efficient internalization of silica-coated iron oxide nanoparticles of different sizes by primary human macrophages and dendritic cells. Toxicol Appl Pharmacol 253:81–93. https://doi.org/10.1016/j.taap.2011.03.011.
11. Kupferschmidt N, Qazi KR, Kemi C, Vallhov H, Garcia-Bennett AE, Gabrielsson S, Scheynius A. 2014. Mesoporous silica particles potentiate antigen-specific T-cell responses. Nanomedicine (Lond) 9:1835–1846. https://doi.org/10.2217/nnm.13.170.
12. Lee S, Yun HS, Kim SH. 2011. The comparative effects of mesoporous silica nanoparticles and colloidal silica on inflammation and apoptosis. Biomaterials 32:9434–9443. https://doi.org/10.1016/j.biomaterials.2011.08.042.
13. Li A, Qin L, Zhu D, Zhu R, Sun J, Wang S. 2010. Signalling pathways involved in the activation of dendritic cells by layered double hydroxide nanoparticles. Biomaterials 31:748–756. https://doi.org/10.1016/j.biomaterials.2009.09.095.
14. Palomaki J, Karisola P, Pylkkanen L, Savolainen K, Alenius H. 2010.

Engineered nanomaterials cause cytotoxicity and activation on mouse antigen presenting cells. Toxicology 267:125–131. https://doi.org/10.1016/j.tox.2009.10.034.
15. Vallhov H, Gabrielsson S, Stromme M, Scheynius A, Garcia-Bennett AE. 2007. Mesoporous silica particles induce size dependent effects on human dendritic cells. Nano Lett 7:3576–3582. https://doi.org/10.1021/nl0714785.
16. Valkov E, Sharpe T, Marsh M, Greive S, Hyvonen M. 2012. Targeting protein-protein interactions and fragment-based drug discovery. Top Curr Chem 317:145–179. https://doi.org/10.1007/128_2011_265.
17. Winter M, Beer HD, Hornung V, Kramer U, Schins RP, Forster I. 2011. Activation of the inflammasome by amorphous silica and TiO_2 nanoparticles in murine dendritic cells. Nanotoxicology 5:326–340. https://doi.org/10.3109/17435390.2010.506957.
18. Chen W, Zhang Q, Kaplan BL, Baker GL, Kaminski NE. 2014. Induced T cell cytokine production is enhanced by engineered nanoparticles. Nanotoxicology 8(Suppl 1):S11–S23. https://doi.org/10.3109/17435390.2013.848302.
19. Nakanishi K, Tsukimoto M, Tanuma S, Takeda K, Kojima S. 2016. Silica nanoparticles activate purinergic signaling via P2X7 receptor in dendritic cells, leading to production of pro-inflammatory cytokines. Toxicol In Vitro 35:202–211. https://doi.org/10.1016/j.tiv.2016.06.003.
20. Beamer CA, Migliaccio CT, Jessop F, Trapkus M, Yuan D, Holian A. 2010. Innate immune processes are sufficient for driving silicosis in mice. J Leukoc Biol 88:547–557. https://doi.org/10.1189/jlb.0210108.
21. Brandenberger C, Rowley NL, Jackson-Humbles DN, Zhang Q, Bramble LA, Lewandowski RP, Wagner JG, Chen W, Kaplan BL, Kaminski NE, Baker GL, Worden RM, Harkema JR. 2013. Engineered silica nanoparticles act as adjuvants to enhance allergic airway disease in mice. Part Fibre Toxicol 10:26. https://doi.org/10.1186/1743-8977-10-26.
22. SanMiguel A, Grice EA. 2015. Interactions between host factors and the skin microbiome. Cell Mol Life Sci 72:1499–1515. https://doi.org/10.1007/s00018-014-1812-z.
23. Belkaid Y, Segre JA. 2014. Dialogue between skin microbiota and immunity. Science 346:954–959. https://doi.org/10.1126/science.1260144.
24. Kato LM, Kawamoto S, Maruya M, Fagarasan S. 2014. The role of the adaptive immune system in regulation of gut microbiota. Immunol Rev 260:67–75. https://doi.org/10.1111/imr.12185.
25. Ruane DT, Lavelle EC. 2011. The role of CD103(+) dendritic cells in the intestinal mucosal immune system. Front Immunol 2:25. https://doi.org/10.3389/fimmu.2011.00025.
26. Naik S, Bouladoux N, Linehan JL, Han SJ, Harrison OJ, Wilhelm C, Conlan S, Himmelfarb S, Byrd AL, Deming C, Quinones M, Brenchley JM, Kong HH, Tussiwand R, Murphy KM, Merad M, Segre JA, Belkaid Y. 2015. Commensal-dendritic-cell interaction specifies a unique protective skin immune signature. Nature 520:104–108. https://doi.org/10.1038/nature14052.
27. Joffre O, Nolte MA, Sporri R, Reis e Sousa C. 2009. Inflammatory signals in dendritic cell activation and the induction of adaptive immunity. Immunol Rev 227:234–247. https://doi.org/10.1111/j.1600-065X.2008.00718.x.
28. Ruane D, Brane L, Reis BS, Cheong C, Poles J, Do Y, Zhu H, Velinzon K, Choi JH, Studt N, Mayer L, Lavelle EC, Steinman RM, Mucida D, Mehandru S. 2013. Lung dendritic cells induce migration of protective T cells to the gastrointestinal tract. J Exp Med 210:1871–1888. https://doi.org/10.1084/jem.20122762.
29. Sabatte J, Maggini J, Nahmod K, Amaral MM, Martinez D, Salamone G, Ceballos A, Giordano M, Vermeulen M, Geffner J. 2007. Interplay of pathogens, cytokines and other stress signals in the regulation of dendritic cell function. Cytokine Growth Factor Rev 18:5–17. https://doi.org/10.1016/j.cytogfr.2007.01.002.
30. Blanco P, Palucka AK, Pascual V, Banchereau J. 2008. Dendritic cells and cytokines in human inflammatory and autoimmune diseases. Cytokine Growth Factor Rev 19:41–52. https://doi.org/10.1016/j.cytogfr.2007.10.004.
31. Di Cristo L, Movia D, Bianchi MG, Allegri M, Mohamed BM, Bell AP, Moore C, Pinelli S, Rasmussen K, Riego-Sintes J, Prina-Mello A, Bussolati O, Bergamaschi E. 2016. Pro-inflammatory effects of pyrogenic and precipitated amorphous silica nanoparticles in innate immunity cells. Toxicol Sci 150:40–53. https://doi.org/10.1093/toxsci/kfv258.
32. Mariathasan S, Weiss DS, Newton K, McBride J, O'Rourke K, Roose-Girma M, Lee WP, Weinrauch Y, Monack DM, Dixit VM. 2006. Cryopyrin activates the inflammasome in response to toxins and ATP. Nature 440:228–232. https://doi.org/10.1038/nature04515.
33. He Y, Franchi L, Nunez G. 2013. TLR agonists stimulate Nlrp3-dependent IL-1beta production independently of the purinergic P2X7 receptor in dendritic cells and in vivo. J Immunol 190:334–339. https://doi.org/10.4049/jimmunol.1202737.
34. Sandberg WJ, Lag M, Holme JA, Friede B, Gualtieri M, Kruszewski M, Schwarze PE, Skuland T, Refsnes M. 2012. Comparison of non-crystalline silica nanoparticles in IL-1beta release from macrophages. Part Fibre Toxicol 9:32. https://doi.org/10.1186/1743-8977-9-32.
35. Sharp FA, Ruane D, Claass B, Creagh E, Harris J, Malyala P, Singh M, O'Hagan DT, Petrilli V, Tschopp J, O'Neill LA, Lavelle EC. 2009. Uptake of particulate vaccine adjuvants by dendritic cells activates the NALP3 inflammasome. Proc Natl Acad Sci U S A 106:870–875. https://doi.org/10.1073/pnas.0804897106.
36. Fedeli C, Segat D, Tavano R, Bubacco L, De Franceschi G, de Laureto PP, Lubian E, Selvestrel F, Mancin F, Papini E. 2015. The functional dissection of the plasma corona of SiO(2)-NPs spots histidine rich glycoprotein as a major player able to hamper nanoparticle capture by macrophages. Nanoscale 7:17710–17728. https://doi.org/10.1039/C5NR05290D.
37. Shi Y, Yadav S, Wang F, Wang H. 2010. Endotoxin promotes adverse effects of amorphous silica nanoparticles on lung epithelial cells in vitro. J Toxicol Environ Health A 73:748–756. https://doi.org/10.1080/15287391003614042.
38. Segat D, Tavano R, Donini M, Selvestrel F, Rio-Echevarria I, Rojnik M, Kocbek P, Kos J, Iratni S, Sheglmann D, Mancin F, Dusi S, Papini E. 2011. Proinflammatory effects of bare and PEGylated ORMOSIL-, PLGA- and SUV-NPs on monocytes and PMNs and their modulation by f-MLP. Nanomedicine (Lond) 6:1027–1046. https://doi.org/10.2217/nnm.11.30.
39. Tavano R, Segat D, Fedeli C, Malachin G, Lubian E, Mancin F, Papini E. 2016. Formyl-peptide receptor agonists and amorphous SiO_2-NPs synergistically and selectively increase the inflammatory responses of human monocytes and PMNs. Nanobiomedicine 3:2. https://doi.org/10.5772/62251.
40. Athinarayanan J, Periasamy VS, Alsaif MA, Al-Warthan AA, Alshatwi AA. 2014. Presence of nanosilica (E551) in commercial food products: TNF-mediated oxidative stress and altered cell cycle progression in human lung fibroblast cells. Cell Biol Toxicol 30:89–100. https://doi.org/10.1007/s10565-014-9271-8.
41. Dekkers S, Krystek P, Peters RJ, Lankveld DP, Bokkers BG, van Hoeven-Arentzen PH, Bouwmeester H, Oomen AG. 2011. Presence and risks of nanosilica in food products. Nanotoxicology 5:393–405. https://doi.org/10.3109/17435390.2010.519836.
42. Bosch A, Maier M, Morfeld P. 2012. Nanosilica? Clarifications are necessary! Nanotoxicology 6:611–613. https://doi.org/10.3109/17435390.2011.595837.
43. Tarantini A, Huet S, Jarry G, Lanceleur R, Poul M, Tavares A, Vital N, Louro H, Joao Silva M, Fessard V. 2015. Genotoxicity of synthetic amorphous silica nanoparticles in rats following short-term exposure. Part 1. Oral route. Environ Mol Mutagen 56:218–227. https://doi.org/10.1002/em.21935.
44. Peters R, Kramer E, Oomen AG, Rivera ZE, Oegema G, Tromp PC, Fokkink R, Rietveld A, Marvin HJ, Weigel S, Peijnenburg AA, Bouwmeester H. 2012. Presence of nano-sized silica during in vitro digestion of foods containing silica as a food additive. ACS Nano 6:2441–2451. https://doi.org/10.1021/nn204728k.
45. Yoshida T, Yoshioka Y, Takahashi H, Misato K, Mori T, Hirai T, Nagano K, Abe Y, Mukai Y, Kamada H, Tsunoda S, Nabeshi H, Yoshikawa T, Higashisaka K, Tsutsumi Y. 2014. Intestinal absorption and biological effects of orally administered amorphous silica particles. Nanoscale Res Lett 9:532. https://doi.org/10.1186/1556-276X-9-532.
46. Rancan F, Gao Q, Graf C, Troppens S, Hadam S, Hackbarth S, Kembuan C, Blume-Peytavi U, Ruhl E, Lademann J, Vogt A. 2012. Skin penetration and cellular uptake of amorphous silica nanoparticles with variable size, surface functionalization, and colloidal stability. ACS Nano 6:6829–6842. https://doi.org/10.1021/nn301622h.
47. Hirai T, Yoshioka Y, Takahashi H, Ichihashi K, Yoshida T, Tochigi S, Nagano K, Abe Y, Kamada H, Tsunoda S, Nabeshi H, Yoshikawa T, Tsutsumi Y. 2012. Amorphous silica nanoparticles enhance cross-presentation in murine dendritic cells. Biochem Biophys Res Commun 427:553–556. https://doi.org/10.1016/j.bbrc.2012.09.095.
48. Hirai T, Yoshioka Y, Takahashi H, Ichihashi K, Udaka A, Mori T, Nishijima N, Yoshida T, Nagano K, Kamada H, Tsunoda S, Takagi T, Ishii KJ, Nabeshi H, Yoshikawa T, Higashisaka K, Tsutsumi Y. 2015. Cutaneous exposure to agglomerates of silica nanoparticles and allergen results in IgE-biased immune response and increased sensitivity to anaphylaxis in mice. Part Fibre Toxicol 12:16. https://doi.org/10.1186/s12989-015-0095-3.

49. Nabeshi H, Yoshikawa T, Matsuyama K, Nakazato Y, Arimori A, Isobe M, Tochigi S, Kondoh S, Hirai T, Akase T, Yamashita T, Yamashita K, Yoshida T, Nagano K, Abe Y, Yoshioka Y, Kamada H, Imazawa T, Itoh N, Tsunoda S, Tsutsumi Y. 2010. Size-dependent cytotoxic effects of amorphous silica nanoparticles on Langerhans cells. Pharmazie 65:199–201.
50. Yoshida T, Yoshikawa T, Nabeshi H, Matsuyama K, Hirai T, Akase T, Yoshioka Y, Itoh N, Tsutsumi Y. 2012. Amorphous nanosilica particles induce ROS generation in Langerhans cells. Pharmazie 67:740–741.
51. Fedeli C, Selvestrel F, Tavano R, Segat D, Mancin F, Papini E. 2013. Catastrophic inflammatory death of monocytes and macrophages by overtaking of a critical dose of endocytosed synthetic amorphous silica nanoparticles/serum protein complexes. Nanomedicine (Lond.) 8:1101–1126. https://doi.org/10.2217/nnm.12.136.
52. Beamer CA, Holian A. 2008. Silica suppresses Toll-like receptor ligand-induced dendritic cell activation. FASEB J 22:2053–2063. https://doi.org/10.1096/fj.07-095299.